Nonlinearly most dangerous disturbance for high-speed boundary-layer transition

Supplementary Material

Reza Jahanbakhshi[1] and Tamer A. Zaki[1]†

[1]Department of Mechanical Engineering, Johns Hopkins University
Baltimore, MD 21218-2682, USA

(Received *; revised *; accepted *)

This document includes movies of numerical Schlieren and figures that lend additional support to the discussions in the main text.

1. Movies from the simulations

The section includes supplemental movies that supports and complements the conclusions in the main paper. The movies depict contours of the numerical Schlieren technique based on the divergence of velocity,

$$\mathcal{S} = c_1 \left[1 - \tanh\left(\frac{c_2 \nabla.\vec{\mathbf{u}}}{|\nabla.\vec{\mathbf{u}}|_{\max}} \right) \right] \tag{1.1}$$

where the subscript"max" denotes the maximum absolute value of velocity divergence over the entire computational field, and c_1 and c_2 are adjustable parameters which control the background color shade and the amplification of small dilatation respectively. In the movies $c_1 = 1$ and $c_2 = 25|\nabla.\vec{\mathbf{u}}|_{\max}$.

Movie # 1: Side view of numerical Schlieren contours from case E1N at $z = L_z/2$.

Movie # 2: Side view of numerical Schlieren contours from case E2N at $z = L_z/4$.

2. Energy spectra from cases E1 and E2

Figure 1 shows the downstream development of energy $\mathcal{E}_{\langle F,k_z\rangle}$ in each of the 400 modes that are prescribed at the inlet, for simulations E1 and E2. In these simulations, the inflow spectra are the optima reached at the final iteration of the EnVar algorithm. Thick coloured curves corresponding to important modes that participate substantively in the transition process, while the remaining modes are shown as thin gray lines.

3. Energy spectra from additional simulations E1L# and E2L

Figure 2 shows the downstream development of the energy $\mathcal{E}_{\langle F,k_z\rangle}$ of selected instability modes from cases E1L1, E1L2, E1L3 and E2L. The inflow conditions for these simulations were motivated by linear stability theory and are reported in table 2 in the main text. In the figure, solid lines correspond to the energy computed from the DNS data, and the selected modes are the main cause of transition in each case. The dashed and dashed-dotted lines are obtained by advancing the modes using the linear parabolized stability equations (PSE), in the first case assuming a Blasius base-state profile and in the second using the distorted mean-flow profile from DNS.

† Email address for correspondence: t.zaki@jhu.edu

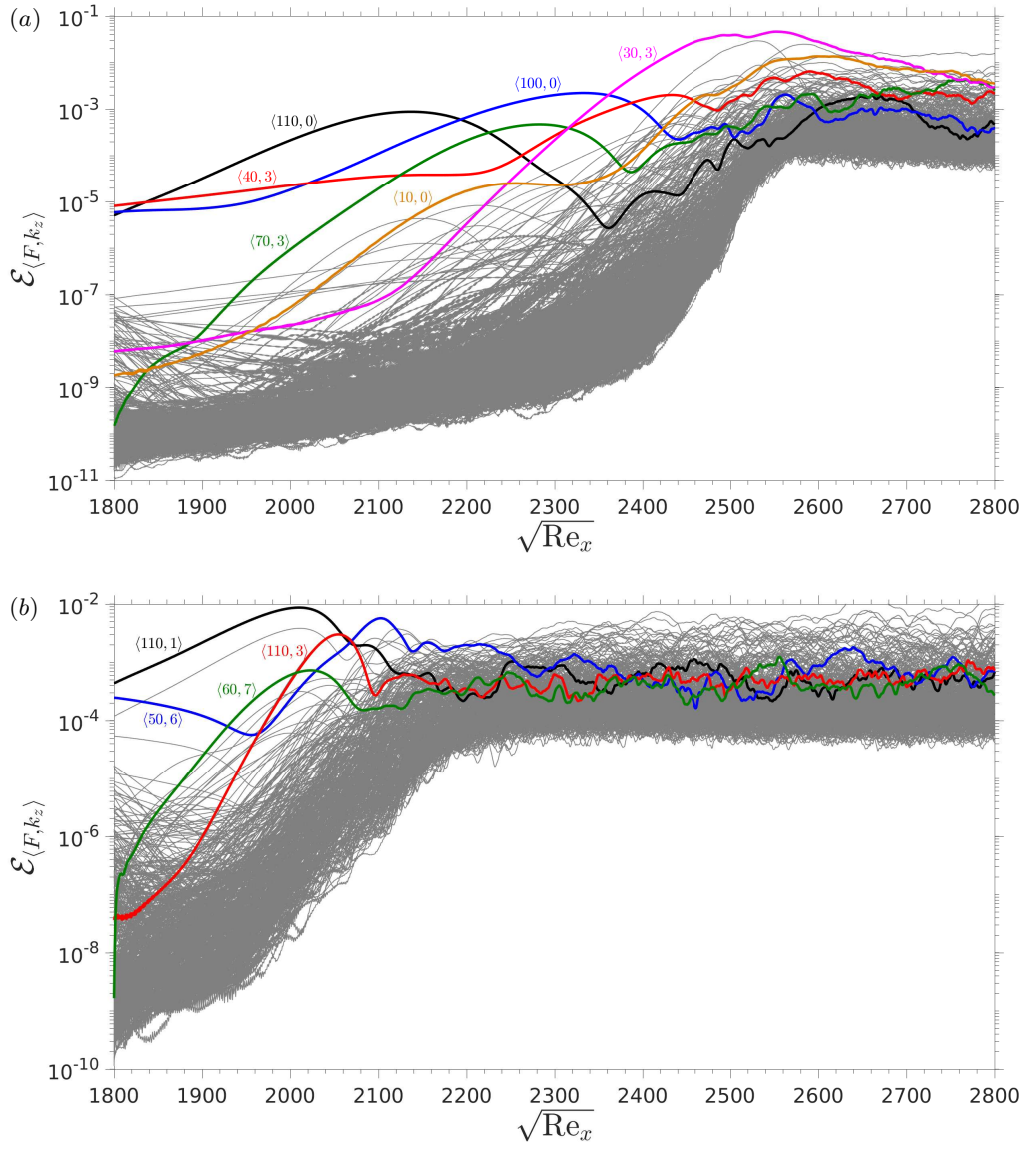

FIGURE 1. Downstream development of the energy of the 400 inlet instability modes in cases (*a*) E1 and (*b*) E2. The spectrum at the inlet in each case is the optimal condition identified by the final iteration of the EnVar algorithm.

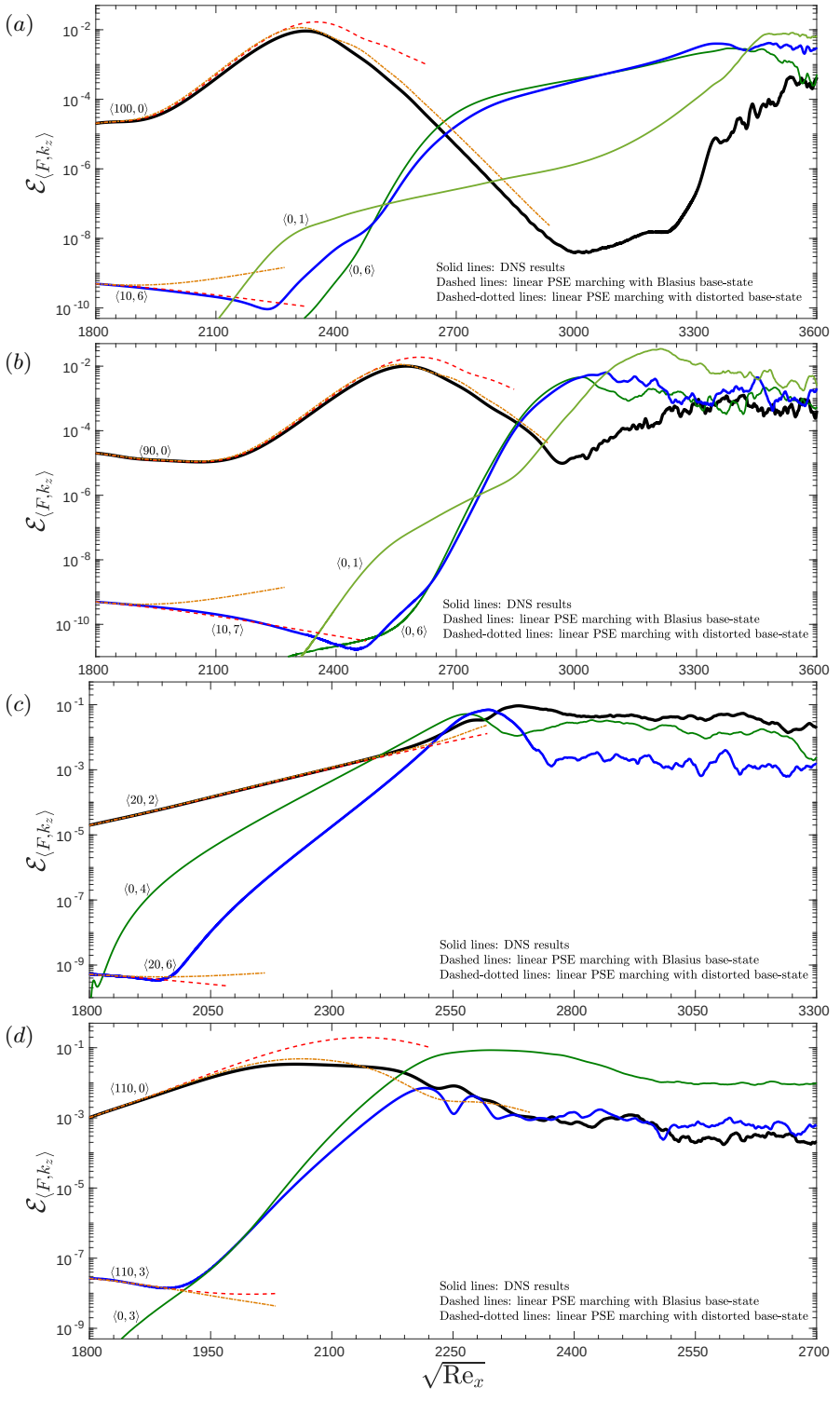

FIGURE 2. Downstream development of the energy of select instability modes $\mathcal{E}_{\langle F,k_z\rangle}$ from cases (*a*) E1L1, (*b*) E1L2, (*c*) E1L3, and (*d*) E2L.